JOURNAL OF COMPUTATIONAL PHYSICS 13, 59–69 (1973)

A Method for Computing the Transition from Ambipolar to Free Diffusion in a Decaying Plasma*

J. R. FREEMAN

Sandia Laboratories, Albuquerque, New Mexico 87115

Received March 13, 1973

A method for economically obtaining accurate results for the transition from ambipolar to free diffusion in an isothermal afterglow is presented. The techniques employ variable spatial zoning for sheath resolution and utilize the Gear package for integrating the stiff system of equations in time. Results are presented which indicate that significant errors can be made by improper sheath resolution. The results also show that in contrast to earlier work, the computational times required are insensitive to the ratio of ion to electron diffusion coefficients.

I. INTRODUCTION

This work reports a method which has been developed to study diffusion processes in decaying plasmas, with particular application to investigating the transition from electron-ion ambipolar diffusion to free diffusion of the separate species. This paper is restricted to the study of the isothermal afterglow confined by a cylindrical chamber, although the techniques are applicable to active plasmas and plasmas with multiple ion species. The earliest work on this topic was reported by Allis and Rose [1], who studied the problem in the context of a steady electron loss rate. The full time dependent problem was first examined by Kregel [2], who compared the time decay of the average electron density with the experiments in helium of Freiberg and Weaver [3]. Gusinow and Gerber [4] reported calculations which specifically compared the steady-state results of Allis and Rose with the full time dependent solutions for both the electrons and ions. Recent experimental comparisons with the calculations of Kregel have been reported by Gerber and Gerardo [5].

The numerical solution for the time dependent problem is greatly complicated by the stiff character of the model equations. The electron and ion diffusion coefficients in helium differ by more than a factor of five hundred, and the initial

* This work was supported by the United States Atomic Energy Commission.

characteristic frequency of the self-consistent electric field at high initial densities exceeds the ambipolar rate by about eight orders of magnitude. Systems of equations with decaying solutions having greatly differing time constants are usually referred to as "stiff." The spatial dependence of the variables also contributes to the difficulties, in that a sheath forms at the wall which at high densities has a thickness of only a few percent of the chamber radius. Since the resolution of this sheath is crucial to the correct computation of the start of the transition regime, it is clear that serious spatial zoning problems exist.

The method of solution reported in this work employs the stiff system solver developed by Gear [6, 7]. This technique permits stable, accurate solutions to be obtained using time steps greatly exceeding those derived for explicit methods. The application of the Gear solver to ordinary differential equations derived from partial differential equations will be discussed. The spatial resolution difficulties were overcome by using a variable zoning density, similar to that reported by Rivas [8]. This type of zoning provides an excellent resolution of the sheath, while still allowing a reasonable zoning of the central region. Results are presented which indicate that the twenty mesh calculation of Kregel leads to an artificially slow electron diffusion rate and to erroneous values for the electric field near the wall. This is a manifestation of an inadequate resolution of the Debye sheath. Comparisions are also made with the computational times reported by Gusinow and Gerber which indicate the rather dramatic reduction in running time available by using the Gear package in conjunction with variable zoning.

II. Basic Equations

We consider an isothermal afterglow confined by an infinitely long cylindrical discharge chamber. The pressure of the neutral gas is assumed high enough to ensure that the mean free-paths are smaller than all relevant dimensions, including the Debye sheath at the wall. For the purposes of this work it is also assumed that the electron and ion densities are zero on the chamber wall. This assumption is consistent with the earlier work [1, 2, 4] with which we wish to compare, although recent calculations [9] consider more realistic conditions for the electron density. Under these assumptions, the equations describing the system are

$$\frac{\partial p}{\partial t} = \frac{D_+}{r}\frac{\partial}{\partial r}\left(r\frac{\partial p}{\partial r}\right) - \frac{\mu_+}{r}\frac{\partial}{\partial r}(rpE), \tag{1}$$

$$\frac{\partial n}{\partial t} = \frac{D_-}{r}\frac{\partial}{\partial r}\left(r\frac{\partial n}{\partial r}\right) + \frac{\mu_-}{r}\frac{\partial}{\partial r}(rnE), \tag{2}$$

$$(1/r(\partial/\partial r)(rE) = (e/\epsilon_0)(p - n), \tag{3}$$

where p and n are the ion and electron densities in particles/m^3, E is the magnitude of the space charge electric field in volts/m, μ and D are the mobilities and diffusion coefficients for the relevant species, e is the electronic charge, and ϵ_0 is the free space permittitivity. Equations (1) and (2) are the species continuity equations and Eq. (3) is the Poisson equation.

The boundary conditions at the chamber wall ($r = r_b$) are that $n(r_b, t) = p(r_b, t) = 0$. At the origin, symmetry considerations imply that

$$\partial n(0, t)/\partial r = \partial p(0, t)/\partial r = E(0, t) = 0.$$

The definition of the problem is completed only upon specification of initial conditions for $n(r, 0)$ and $p(r, 0)$, typically of the form $p(r, 0) = n(r, 0) = n_0 J_0(r/\Lambda)$, where $\Lambda \equiv r_b/\alpha_1$ and α_1 is the first zero of the zero order Bessel function. It is important to use values of n_0 sufficiently large to insure that the computations begin well in the ambipolar region, so that the somewhat arbitrary initial conditions do not affect the transition behavior.

Equations (1)–(3) can be combined to yield an alternate form for the electric field equation, given by

$$\partial E/\partial t = (e/\epsilon_0)[D_+(\partial p/\partial r) - D_-(\partial n/\partial r) - (\mu_+ p + \mu_- n) E], \tag{4}$$

which can be used instead of Eq. (3). This alternative is attractive because of its similarity in form to Eqs. (1) and (2), allowing the reduction of all three equations to a first order system of ordinary differential equations in time. It should be pointed out that the use of Eq. (4) requires some care in the spatial zoning to obtain numerical results consistent with Eq. 3. The difference form to be described satisfied this consistency check to at least seven digits for all cases examined.

The stiffness of the system can be seen easily by examining some typical numbers for a helium afterglow as used by Kregel [2]. Diffusion coefficients at a pressure of 4.0 torr are given approximately by $D_+ = 9.8 \times 10^{-3}$ m^2/sec for He_2^+ and $D_- = 5.14$ m^2/sec. Since the characteristic free diffusion times for the species are given by $\tau = \Lambda^2/D$, we see that electrons tend to diffuse over 500 times faster than the ions. Initial densities as high as $n_0 = 10^{17}\, m^{-3}$ are indicated by Kregel. An approximate time constant for the initial growth of the electric field at this density can be obtained by retaining only the largest term on the right hand side of Eq. (4), leading to a characteristic time $\tau_E \sim \epsilon_0/e\mu_- n_0 \simeq 10^{-12}$ sec. For a wall radius $r_b = 4 \times 10^{-3}$ m, the characteristic time for ambipolar diffusion is given by $\tau_A = \Lambda^2/2D_+ \simeq 10^{-4}$ sec. Transient responses to density perturbations at high densities occur on the τ_E time scale, which is very small compared to τ_A.

The spatial zoning difficulty is evident upon comparing the Debye length, $\lambda_D = (\epsilon_0 kT/n_0 e^2)^{1/2} \simeq 3.7 \times 10^{-6}$ m, with the chamber radius $r_b = 4 \times 10^{-3}$ m. A value of ($kT/e = D/\mu = 0.025$) for both species was used for this comparison. The actual wall sheath can be as large as ten or twenty Debye lengths, since the

density near the wall is much lower than the central density. Nevertheless, these considerations preclude the use of standard numerical techniques for obtaining accurate results in a reasonable time.

III. Spatial Differencing

The right-hand side of Eqs. (1), (2), and (4) will be represented by a finite difference form using nonuniform zoning. The zone interfaces will be denoted by r_j, $1 \leqslant j \leqslant N$, where $r_1 = 0$ and $r_N = r_b$. The electric field will be defined at the zone interfaces, while the particle densities will be defined at points internal to the zones, given by $\bar{r}_j$, $1 \leqslant j \leqslant N$. The extra zone point at $\bar{r}_N$ is used to provide a mesh point outside of the chamber wall to satisfy the wall boundary condition, i.e., $n(\bar{r}_N) = -n(\bar{r}_{N-1})$, so that $n(r_b) = 0$, since $r_b = (\bar{r}_N + \bar{r}_{N-1})/2$. We adopt the specification that the zone interfaces and internal mesh points are related by

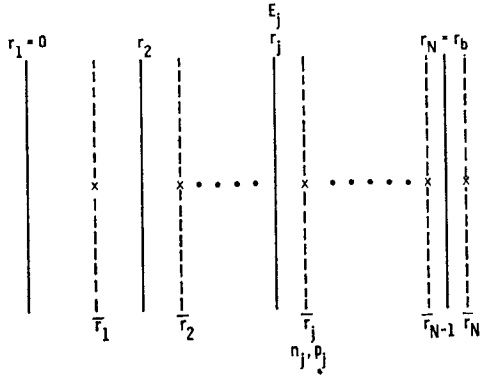

FIG. 1. Spatial zoning arrangement. The zone boundaries are shown by the solid lines and the points where the densities are calculated by the dashed lines.

$r_j = (\bar{r}_{j-1} + \bar{r}_j)/2$, $2 \leqslant j \leqslant N$. This configuration is shown in Fig. 1. Using these definitions, the spatially differenced form of Eq. (1) can be written as

$$\partial p_j/\partial t = D_+[(p_{j+1} - p_j)(1 + \Delta^-/2\bar{r}_j)/\Delta^+ - (p_j - p_{j-1})(1 - \Delta^+/2\bar{r}_j)/\Delta^-]/\Delta_{\text{ave}} - \mu_+[\hat{p}_{j+1}(1 + \Delta^-/2\bar{r}_j)\, E_{j+1} - \hat{p}_j(1 - \Delta^+/2\bar{r}_j)\, E_j]/\Delta_{\text{ave}}, \quad (5)$$

where

$$\Delta^+ = \bar{r}_{j+1} - \bar{r}_j,$$
$$\Delta^- = \bar{r}_j - \bar{r}_{j-1},$$
$$\Delta_{\text{ave}} = (\Delta^+ + \Delta^-)/2,$$

and

$$\hat{p}_j = (p_j + p_{j-1})/2,$$

i.e., $\hat{p}_j$ is the density interpolated to the r_j mesh interfaces. The simple form for $\hat{p}_j$ is a benefit arising from the definition of $r_j = (\bar{r}_{j-1} + \bar{r}_j)/2$. The difference equation for the electron density can be obtained simply from Eq. (5) by replacing all p's with n's, replacing D_+ with D_-, and μ_+ with the negative value of μ_-. The electric field equation is written as

$$\partial E_j/\partial t = (e/\epsilon_0)\{[D_+(p_j - p_{j-1}) - D_-(n_j - n_{j-1})]/\Delta^- - (\mu_+ \hat{p}_j + \mu_- \hat{n}_j) E_j\}. \quad (6)$$

The truncation error of Eq. (5) can be examined by expanding the variables in Taylor series about the point $\bar{r}_j$. Substitution into Eq. (5) yields

$$\begin{aligned}\frac{\partial p}{\partial t}\Big|_{\bar{r}_j} = &\left[\frac{D_+}{r}\frac{\partial}{\partial r}\left(r\frac{\partial p}{\partial r}\right) - \frac{\mu_+}{r}\frac{\partial}{\partial r}(rpE)\right]\Big|_{\bar{r}_j} \\ &+ \left\{\frac{\partial^3 p}{\partial r^3}\cdot(D_+(\Delta^+ - \Delta^- + \Delta^+\Delta^-/2\bar{r}_j)/3)\right. \\ &\left. - \left[\frac{E\,\partial^2 p}{\partial r^2} + \frac{\partial^2(Ep)}{\partial r^2}\right]\cdot\mu_+(\Delta^+ - \Delta^- + \Delta^+\Delta^-/2\bar{r}_j)/4\right\}\Big|_{\bar{r}_j} \\ &+ \text{higher order terms.} \end{aligned} \quad (7)$$

Similarly, Eq. (6) becomes

$$\begin{aligned}\frac{\partial E}{\partial t}\Big|_{r_j} = \frac{e}{\epsilon_0}&\left\{\left[D_+\frac{\partial p}{\partial r} - D_-\frac{\partial n}{\partial r} - (\mu_+ p + \mu_- n)\,E\right]\Big|_{r_j}\right. \\ &+ \left[\left(\left(D_+\frac{\partial^3 p}{\partial r^3} - D_-\frac{\partial^3 n}{\partial r^3}\right)\Delta^{-2}/24\right) - \left(\mu_+\frac{\partial^2 p}{\partial r^2} + \mu_-\frac{\partial^2 n}{\partial r^2}\right)E\Delta^{-2}/8\right]\Big|_{r_j} \\ &\left. + \text{higher order terms}\right\}. \end{aligned} \quad (8)$$

It is seen from Eq. (8) that our arrangement of zones yields second order accuracy for the field equation, even with variable zoning. The truncation terms of Eq. (7) remain to first order near the origin even for uniform zoning, since $\bar{r}_j$ is of order Δ in this region. This restricts our variable zoning arrangements to schemes which not only resolve the wall sheath, but also retain good resolution near the origin. It is also seen from Eq. (7) that the use of nonuniform zoning adds truncation terms proportional to $[\Delta^+ - \Delta^-]$. A zoning arrangement designed specifically for this type of error has been described by Rivas [8]. It is based on the philosophy that the fractional change in adjacent zone widths will be restricted in regions of large Δ, but large fractional changes will be allowed when the zone size is very small anyway. The zoning arrangement to be used results in reducing $[\Delta^+ - \Delta^-]$ to second order in the maximum Δ over the entire domain of the problem. It also

provides many zones near the chamber wall without destroying the resolution of the central region. The particular form suggested by Rivas, and used in this work, defines the interior mesh points $\bar{r}_j$ as

$$\bar{r}_j = [1 - (1 - j/N)^2]\, r_b\,, \qquad 1 \leqslant j \leqslant N - 1. \tag{9}$$

The extra zone outside of the boundary is given by $\bar{r}_N = 2r_b - \bar{r}_{N-1}$, and the zone interface locations follow from the earlier definition-of $r_j = (\bar{r}_{j-1} + \bar{r}_j)/2$. Near the origin, Eq. (9) provides a zone spacing of about $2r_b/N$, which is only twice as coarse as that arising from uniform zoning. Near the wall, the zone width decreases to about r_b/N^2, providing excellent resolution of the wall sheath.

The computation of variables at the boundaries requires only a slight alteration of the basic scheme. The additional mesh point of $\bar{r}_N$ is loaded with density values $(-p_{N-1})$ and $(-n_{N-1})$, so that $\hat{p}_N = \hat{n}_N = 0$ at $r = r_b$. The condition that $\partial p/\partial r = 0$ at the origin is satisfied by letting $p_{j-1} = p_j$ in Eq. (5) when $j = 1$. A similar form is used for computing n_j for $j = 1$.

IV. Integration in Time

The set of simultaneous equations defined by Eq. (5) for p and its analog for n, plus Eq. (6) for the electric field, can be considered to be a set of $3N$ ordinary differential equations with time as the independent variable. This system has the form

$$d\mathbf{W}/dt = f(\mathbf{W}), \tag{10}$$

where the vector $\mathbf{W}$ contains the $3N$ elements arising from defining p, n, and E at N mesh points.

This form is particularly suited for integration using the method of Gear [6, 7]. This technique was derived specifically for stiff systems, and has been successfully incorporated into the present work. The Gear method, using a variable time step and a variable order implicit predictor–corrector scheme, incorporates no formal time step restriction based on zone size. This capability is crucial in allowing the use of fine zoning in the sheath region without the usual time step reduction. As a result, the nonuniformly zoned results to be presented were completed with almost no running time increase over uniformly zoned cases.

The Gear package provides for convergence requirements based on either a relative or absolute local error estimate. Since accurate computations were required even for small ion and electron densities, a relative local error requirement was used for all variables. When the central electron density had decreased by seven orders of magnitude, the electron density equations were no longer computed,

permitting the calculations to continue on the ion free diffusion time scale. Most of the runs to be presented used a relative error criterion of 10^{-4}. Cases run with an error of 10^{-6} showed a negligible difference.

V. Results

Before concentrating on actual ambipolar diffusion problems, initial runs were made in which the electric field was forced to remain equal to zero for all time. It is seen from Eqs. (1) and (2) that the ions and electrons will simply diffuse freely, providing a test case having an analytic solution. For initial density distributions $p_0 J_0(r/\Lambda)$ and $n_0 J_0(r/\Lambda)$ the time dependent solution is given by

$$p(r, t) = p_0 J_0(r/\Lambda)\, e^{-t/\tau_p},$$
$$n(r, t) = n_0 J_0(r/\Lambda)\, e^{-t/\tau_n},$$

where $\Lambda = r_b/\alpha_1$, α_1 is the first zero of the Bessel function, and $\tau_p = \Lambda^2/D_+$, $\tau_n = \Lambda^2/D_-$.

Runs were made with both uniform zoning and the variable zoning of Eq. (9) to check for differences in the accumulated error. The first run used twenty uniformly spaced zones to compute the free diffusion for a time equal to $16\tau_p$, corresponding to a reduction of the central ion density by seven orders of magnitude. The central density at this time differed from the analytic result by only 1.3%, indicating no significant error accumulation. The same case was run for twenty zones arranged nonuniformly using the scheme of Eq. (9). The error at $t = 16\tau_p$ was 1.7%, indicating that the nonuniform zoning provided answers substantially as accurate as the uniformly zoned case, at least for this particular test problem.

Since the work of Kregel [2] presented the first time dependent solutions to this set of equations, and since his work has been used in recent experimental comparisons [5], an identical case using twenty uniformly spaced meshes was run. The computed results obtained reproduced those of Kregel within the resolution of his published data. This correlation permitted further runs to be made in which only the zoning of the problem was changed. Figure 2 plots the electron density averaged over the cylindrical cross section as a function of time. Only the electron density was plotted because of its greater sensitivity to the zoning. Results are shown for twenty uniform zones, and for twenty, forty, and eighty meshes arranged according to Eq. (9); only points differing significantly from each other are plotted.

Significant differences between the twenty uniform mesh results and the more finely zoned cases begin to occur at average densities of about 10^{14} m^{-3}. The uniformly zoned case leads to an artificially slower electron diffusion during the transition, resulting in errors of around an order of magnitude at the lowest

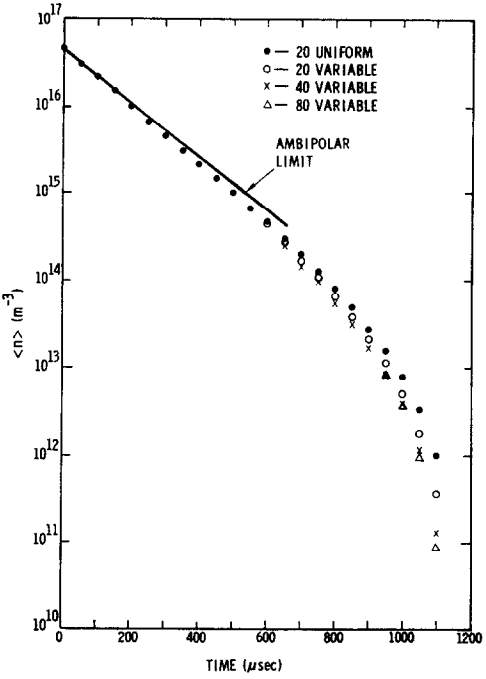

FIG. 2. Decay of average electron density as a function of time.

densities plotted. The twenty mesh variably zoned case leads to a higher electron loss rate, but forty zones are required to permit accurate calculations for a density reduction of five orders of magnitude. Significant differences between the eighty and forty mesh variably zoned cases are seen only for density reductions of greater than 10^5. Typical running times on the CDC-6600 for the twenty, forty, and eighty mesh cases were two, ten, and sixty minutes, indicating that the forty mesh case provides the best compromise between running time and accuracy. A similar plot for the unaveraged central density as a function of time showed a similar behavior.

We next consider possible reasons why the uniformly zoned case leads to a slower electron diffusion. Figure 3 plots the electric field magnitude at the outer wall as a function of average electron density. Only the more accurately zoned cases lead to field values which are only weakly density dependent at high density values, in agreement with the asymptotic results of Allis and Rose [1]. The high electric field arising in the uniformly zoned case tends to attract electrons toward the center, leading to the slower diffusion rate. Other more indirect effects of zoning resolution may also alter the diffusion velocities.

It may be questioned whether an accurate value for the field on the wall is really

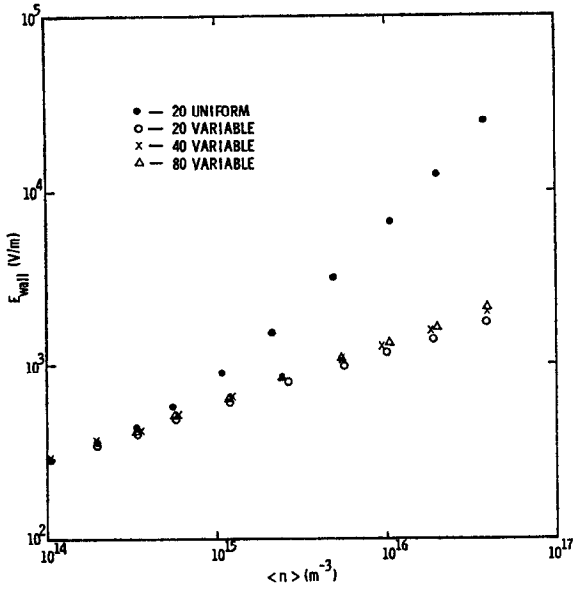

FIG. 3. Wall electric field as a function of average electron density.

required, since Eqs. (1), (2), and (4) show that only the product of the density (assumed zero at the wall) and the field appears in the equations. Although not plotted, significant electric field errors occur just inside the wall. More recent work [9] has been aimed at relaxing the zero density condition for the electrons at the wall and incorporating a boundary condition on the electron current, as suggested by Ingold [10]. This type of boundary condition depends critically on the wall field, since $n \cdot E$ becomes nonzero at r_b.

Since the large electric field can lead to a slower electron diffusion, the source of the high field must be examined. Figure 4a shows the structure of the wall sheath at an average electron density of 10^{16} m^{-3} for the twenty uniformly spaced mesh case. Figure 4b presents the same results for forty variably spaced zones. It can be seen that the uniformly zoned case forces a sheath thickness of at least one zone, even though the correct sheath thickness may be smaller. This forces the quantity $(p - n)$ to be nonzero over an unrealistically large distance, which, as is seen from Eq. (3), results in the higher electric field. It is worth noting that for the uniformly zoned case, the wall field determined by Eq. (4) is inconsistent by about fifty percent with that determined by Eq. (3), again indicating the inadequate sheath resolution. The forty mesh case provides consistency to over four digits even at these high average densities.

The work of Gusinow and Gerber [4] clearly indicates the difficulties which the

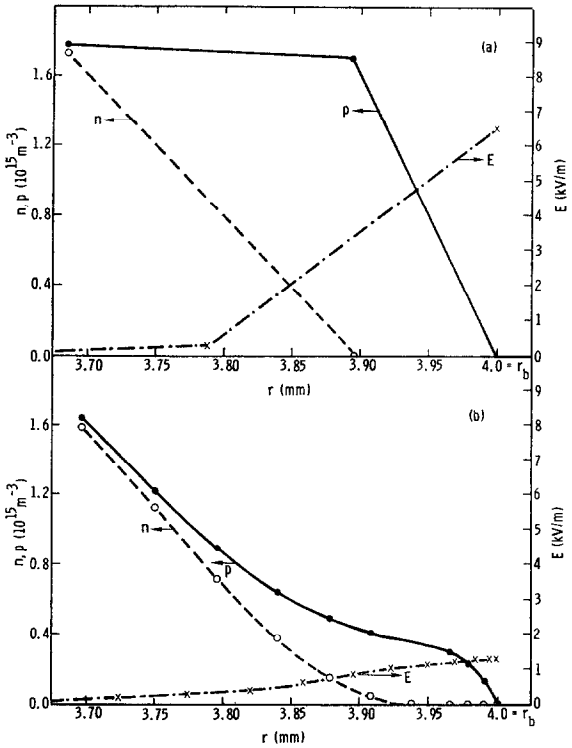

FIG. 4. Radial dependence of sheath structure, for (a) twenty uniformly spaced zoning and (b) forty variably spaced zones. Solid curves are used for ion density, dashed curves for electron density, and dash–dot curves for electric field. Curves are shown for an average electron density of 10^{16} m^{-3}.

standard alternating-direction-implicit methods encounter at high ratios of $S = D_-/D_+$. As the electrons are allowed to be more mobile relative to the ions, the required time step becomes an increasingly smaller fraction of the characteristic ion diffusion time. The published results of Ref. [4] state that while six minutes of CDC-6600 time were used at $S = 32$, the running time increased to sixty-six minutes at $S = 100$.

The method which has been described was used to reproduce the results of [4]. It was found that for $S = 32$, the forty variably spaced zone version produced results to the same accuracy as the 300 zone version of [4]. The more complex techniques used led to a running time of 4.7 minutes, a rather insignificant improvement. Repeating the computations for $S = 100$ required only 5.2 min, an improvement of over an order of magnitude. A further run at $S = 1000$ required 6.3 min, demonstrating the relative insensitivity of the Gear method to increased stiffness.

The success of the present calculations for very stiff problems ($S > 500$) arises from both the variable zoning and the use of the Gear package. It would be informative to know the precise contributions of each of these techniques to the overall improvement. Roughly 120 uniformly spaced zones would be required to obtain the sheath resolution shown in Fig. 4b for forty variably spaced zones. The computer time expended would increase from eleven minues to about three hours. Variable zoning thus forms a crucial part of the method. Attempts to obtain stable, accurate results using standard ADI techniques for very stiff cases with $S > 500$, even with only forty meshes, have led to hopelessly long running times. The Gear package permits the large time steps required for a practical solution.

VI. Summary

A method for computing the transition from ambipolar to free diffusion has been described. The method uses variably spaced zones to provide good sheath resolution, and permits the use of large time steps by means of the Gear stiff system solver. The results obtained indicate that serious errors arise when an insufficient number of zones are used for the sheath region. Results have been presented which demonstrate that the time required for solutions is quite insensitive to the ratio $S = D_-/D_+$, in contrast to earlier work. This flexibility will permit the economical study of various alternative boundary conditions or physical processes in decaying plasma problems.

Acknowledgments

The author would like to thank Drs. R. A. Gerber and M. A. Gusinow for suggesting this work and providing continued encouragement. Much insight and many helpful discussions were contributed by F. O. Lane.

References

1. W. P. Allis and D. J. Rose, *Phys. Rev.* **93** (1954), 84.
2. M. D. Kregel, *J. Appl. Phys.* **41** (1970), 1978.
3. R. J. Freiberg and L. A. Weaver, *Phys. Rev.* **170** (1968), 336.
4. M. A. Gusinow and R. A. Gerber, *Phys. Rev.* **5** (1972), 1802.
5. R. A. Gerber and J. B. Gerardo, *Phys. Rev.* **7A** (1973), 781.
6. C. W. Gear, *Comm. ACM*, **14** (1971), 176.
7. R. J. Gelinas, *J. Comp. Phys.* **9** (1972), 222.
8. E. Kálnay de Rivas, *J. Comp. Phys.* **10** (1972), 202.
9. J. R. Freeman and R. A. Gerber, to be published.
10. J. H. Ingold, *Phys. Fluids* **15** (1972), 75.